




Research Article

# Simultaneous electro-generation and electro-deposition of copper oxide nanoparticles on glassy carbon electrode and its sensor application



R. Shashanka<sup>1</sup>  · B. E. Kumara Swamy<sup>2</sup>

Received: 5 March 2020 / Accepted: 15 April 2020 / Published online: 24 April 2020  
© Springer Nature Switzerland AG 2020

## Abstract

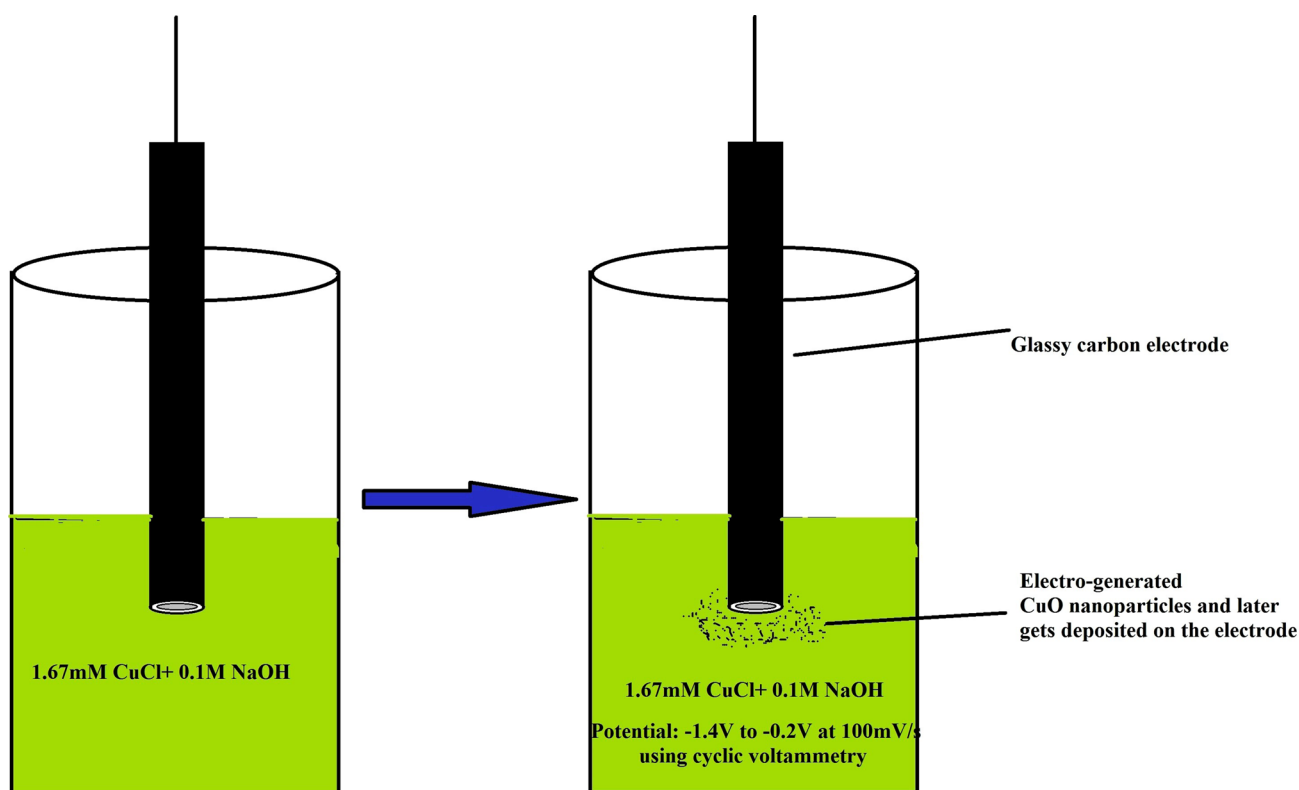
Copper oxide nanoparticles (CuO) were electro-generated and electro-deposited simultaneously on the glassy carbon electrode (GCE) using cyclic voltammetry at a reduction potential of  $-1.4\text{ V}$  to  $-0.2\text{ V}$  in  $0.1\text{ M NaOH}$  and  $1.67\text{ mM CuCl}$  solution. The electrodeposited CuO nanoparticles show an excellent electro-catalytic activity towards the detection of potassium ferricyanide. The scan rate, concentration of the analyte and pH of the solution were varied accordingly to study the stability of the copper oxide deposited glassy carbon electrode (CuO/GCE). The CuO/GCE electrode shows amazing stability, charge transfer and reproducibility even at low concentration of the analyte. The cyclic voltammetry is proved to be one of the convenient methods to reduce the precursors into metal oxide nanoparticles just by applying suitable current. The main advantage of this method is uniform deposition of CuO nanoparticles on GCE and thus increases the number of active sites, surface area and electro-catalytic properties. Scanning electron microscopy (SEM) was used to study the morphology of the electro-generated CuO nanoparticles. The zeta-potential analysis was carried out to study the surface potential of charged CuO nanoparticles and it was found to be  $+58.29\text{ mV}$ . Further, CuO nanoparticles were characterized by X-ray diffraction to study the phases. UV-visible spectroscopy depicts the absorption peak at  $288\text{ nm}$  confirms the formation of CuO nanoparticles. This absorption is attributed by the electronic transition from valence band to conduction band due to the quantum size of the particles.

✉ R. Shashanka, shashankaic@gmail.com | <sup>1</sup>Department of Metallurgical and Materials Engineering, Bartin University, Bartin 74100, Turkey. <sup>2</sup>Department of P.G. Studies and Research in Industrial Chemistry, Kuvempu University, Jnana Sahyadri, Shankaraghatta, Shimoga, Karnataka 577451, India.



SN Applied Sciences (2020) 2:956 | <https://doi.org/10.1007/s42452-020-2785-1>

## Graphical abstract



### Electro-generation and electro-deposition of CuO nanoparticles

**Keywords** Electro-generation · Copper oxide nanoparticles · Glassy carbon electrode · Potassium ferricyanide · Cyclic voltammetry

## 1 Introduction

Nanotechnology has become a hot research area for many researchers working in chemistry, physics, materials science, biomaterials field etc. due to the excellent and unique properties of nanomaterials [1]. In recent past, the researchers showing a substantial interest in metal oxide nanoparticles due to their unusual, unique and remarkable properties due to very fine size [2–5]. It has been reported that as the particle size of the nanomaterials decreases; then most of their properties like catalytic properties [6, 7], mechanical reinforcement [8], electrical conductivity [9], photo catalytic activity [10], hardness, strength of metals and alloys [11, 12] and super paramagnetic properties of magnetic oxides [13] will change significantly. Due to quantum confinement; the nanoparticles show strange optical and electrical properties [14]. Dispersion of these nanoparticles in lesser quantity in various fluids allows

the fabrication of corrosion resistant coatings, electro-catalysts and thin films.

In the present paper we reported a successful electro-generation of CuO nanoparticles and their simultaneous deposition on the glassy carbon electrode using cyclic voltammetry. We investigated the electro-catalytic properties of fabricated CuO/GCE against potassium ferricyanide. Generally, nanoparticles exhibit high energy, surface area and therefore most of them are used as electro-catalysts. Usually the catalytic performance of nanoparticles mainly depends upon their size and shapes [15–18]. Designing of a structurally and dimensionally stable nanoparticle is a difficult job. But this can be achieved by depositing nanoparticles on a suitable support by direct electrochemical method. Cyclic voltammetry is common and popular electro chemical method used to deposit nanoparticles on working electrode [19–25]. In this method, nanoparticles were reduced on electrode in a relatively convenient way by applying suitable current. Compared to other

traditional methods cyclic voltammetry proved to be one of the suitable method to deposit nanoparticles uniformly on the electrode which closely integrate with electrode [26–37]. This increases the number of active sites, surface area and thus increases the catalytic property of the deposited nanoparticles.

Potassium ferricyanide is a bright red colour octahedral coordination compound soluble in water and its solution shows green yellow fluorescence [38]. It is used in a dot etching process as an oxidizing agent to remove silver from negatives and positives; and in colour photograph to reduce the size of colour dots without reducing their numbers. It is also used to increase the solution redox potential ( $E^\circ \approx 436$  mV at pH 7) in physiological experiments [39]. Potassium ferricyanide is the commonly present in the bleaching powder, and it is toxic to the environment. The fabricated electrode can be used to determine the potassium ferricyanide present in the real samples.

S.D. Bukkitgar et al. fabricated graphene oxide (ErGO) and ruthenium doped  $\text{TiO}_2$  nanoparticles based electrode to detect amroxol drug using cyclic voltammetry. They reported the sensor activity at different scan rates, pH and concentration; and also used this method to determine the amroxol content in pharmaceutical dosage forms and in human urine samples [40].

Manasa et al. prepared zinc oxide reduced graphene nanocomposite and cetyltrimethylammonium bromide to detect Bisphenol F. They reported that, the fabricated electrode shows excellent sensitivity, rapid and easy renewal of the electrode surface, short accumulation time and good reproducibility [41].

Rahbar et al. prepared CuO nanoparticles modified carbon paste electrode for the detection of Atrazine using cyclic voltammetry. They reported that, decrease in peak current is proportional to Atrazine concentration in the range of 5–75 ng/mL and the limit of detection and quantification were found to be 2 and 5.6 ng/mL respectively [42].

Amra et al. fabricated CuO modified carbon paste electrode for the detection of detection of Isoproturon in water. Their experimental results proved that, the fabricated electrode showed significant analytical performances over a large quantification range from 1 to 200  $\mu\text{g/L}$  with a detection limit of 0.1  $\mu\text{g/L}$  [43].

Therefore, we reported the fabrication of stable electrode by electrodepositing the electro-generated copper oxide nanoparticles simultaneously on the surface of glassy carbon electrode and also to study the electrochemical behaviour of potassium ferricyanide in different concentrations, pH and scan rates.

## 2 Experimental

### 2.1 Reagents required

Analytical grade CuCl, KCl, NaOH and potassium ferricyanide were purchased from Himedia. All the stock, standard and working solutions were prepared using double distilled water. KCl and NaOH solutions were used as electrolytes.

### 2.2 Instrumentation

The electrochemical work station CHI-660c model was used to carry out all the electrochemical measurements. It is a three electrode electrochemical cell system containing a working electrode (glassy carbon electrode) of 3 mm diameter, a platinum wire as counter electrode and a reference electrode containing Ag/AgCl saturated KCl. Scanning electron microscopy (SEM) was carried out using a Hitachi JSM 1500 (Hitachi, Japan). X-ray diffraction study was performed in PANalytical Xpert Pro XRD. UV–Visible spectral analysis was performed using Perkin Elmer UV–Visible spectrophotometer and zeta potential was measured in Zeta trac-microtrac (Malvern, USA).

## 3 Results and discussion

### 3.1 Preparation of copper oxide nanoparticles modified glassy carbon electrode

The electrode surface was carefully cleaned and polished with aluminium (0.05 mm diameter) powder on polishing

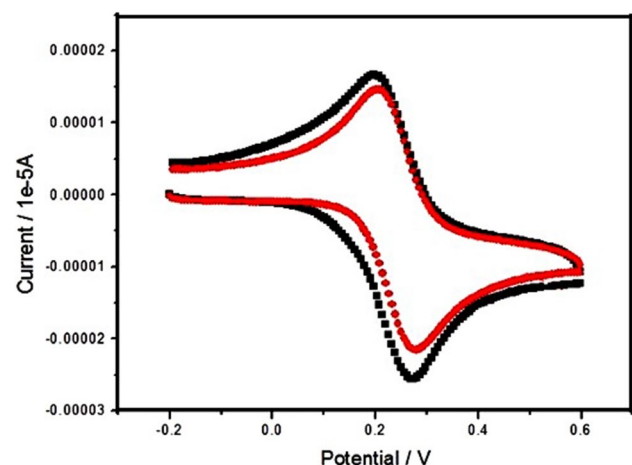


Fig. 1 Cyclic voltammogram of Bare GC and Nano CuO modified GC in 25 Mm Potassium ferricyanide and 1 M KCl at sweep rate of 0.1 V/s

cloth followed by sonication in ethanol, dilute nitric acid (1:1, v/v) and double distilled water individually for 5 min. Finally, the electrode surface was dried by purging high purity  $N_2$  (99.99%). Initially the current sensitivity for bare glassy carbon electrode (BGCE) has been determined using 2 mM Potassium ferricyanide as analyte and 1 M KCl as supporting electrolyte by maintaining the potential of  $-0.2$  V to  $0.6$  V. Then CuO nanoparticles are electro-generated and deposited simultaneously on glassy carbon electrode by applying the reduction potential of  $-1.4$  V to  $-0.2$  V in  $0.1$  M NaOH containing  $1.67$  mM CuCl solution at  $100$  mV/s. The current sensitivity of CuO/GCE is determined by analyzing the analyte potassium ferricyanide in  $1$  M KCl with a potential of  $-0.2$  V to  $0.6$  V. The

cyclic voltammogram obtained for BGCE and CuO/GCE are shown in Fig. 1. From the figure it is confirm that, CuO/GCE show higher sensitivity than BGCE in analyzing potassium ferricyanide in the same experimental conditions. This confirms the deposition of CuO nanoparticles on glassy carbon electrode shows good sensitivity in detecting potassium ferricyanide. We also calculated the exposed surface area of the electrode using Randles–Sevcik equation and the value was found to be  $2.9$  mm<sup>2</sup>.

The potential cycles plays an important role in depositing uniform, optimum thickness of CuO nanoparticles on the electrode. Hence we deposited CuO nanoparticles on glassy carbon electrode at 0, 5, 10, 15 and 20 cycles to get better, uniform, optimum thickness of CuO nano film

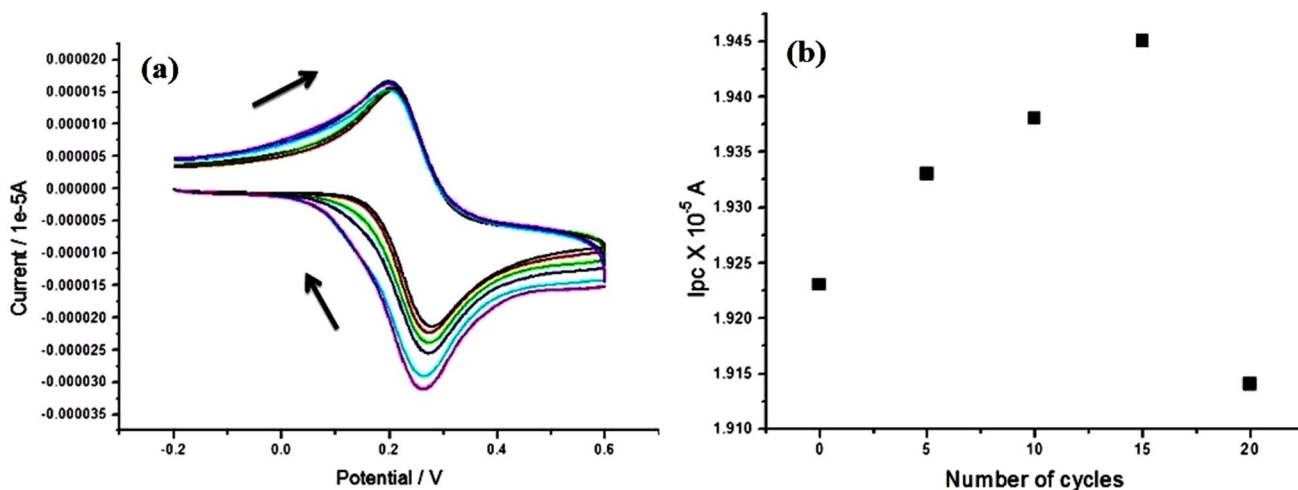


Fig. 2 a Cyclic voltammograms for the effect of variation in the number of cycles from 0, 5, 10, 15 and 20 cycles at  $0.1$  V/s b Graph of Number of cycles versus cathodic peak

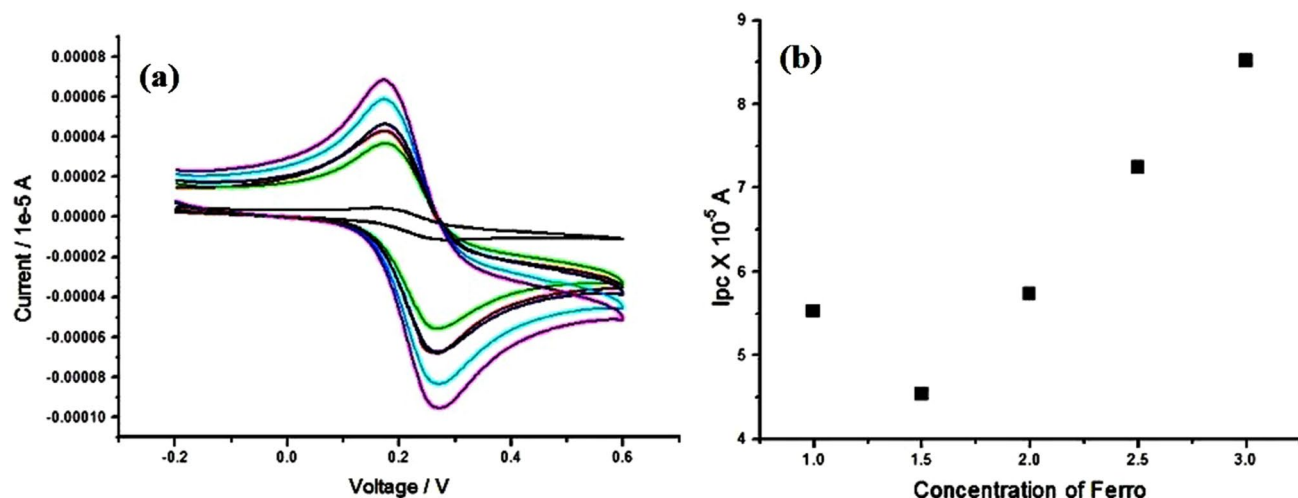


Fig. 3 a Cyclic voltammograms obtained for different concentration of potassium ferricyanide (1 to 3 mM) in  $1$  M KCl solution at scan rate  $100$  mV/s b Graph of concentraion of the potassium ferricyanide vs Cathodic peak current

on electrode to increase the sensitivity of CuO/GCE. After each number of potential cycles, the current sensitivity of CuO/GCE is measured and after each measurement the electrode surface is cleaned carefully with distilled water and polished with aluminium (0.05 mm diameter) slurry on polishing cloth followed by sonicating in ethanol and doubly distilled water (1:1, v/v) for 5 min. Again deposited CuO nanoparticles on the electrode and studied the current sensitivity phenomenon by the same procedure but at different potential cycles. Figure 2a and b show cyclic voltammograms at different number of potential cycles and a graph of cathodic peak current versus number of cycles. We obtained the maximum cathodic peak current of 19.46  $\mu\text{A}$  after 15 cycles and 19.14  $\mu\text{A}$  after 20 cycles. Here, the cathodic peak current increases up to 15 cycles and then suddenly decreases at 20 cycles due to decrease in the active sites and surface area of deposited CuO nanoparticles at 20 cycles. Hence CuO/GCE shows greater stability and sensitivity after 15 potential cycles and therefore we used this electrode for further experimental studies.

### 3.2 Effect of concentration variation of potassium ferricyanide

B. N. Chandrashekar et al. reported the increase of redox peak current with increase in the concentration of most of the analytes [44]. Therefore we studied the effect of different concentration of potassium ferricyanide on the cathodic peak current of CuO/GCE by using cyclic voltammetry. Concentration of only potassium ferricyanide is increased from 1 to 3 mM by keeping the supporting

electrolyte concentration constant (1 M KCl). Figure 3a shows cyclic voltammogram of 1 to 3 mM concentration of potassium ferricyanide in 1 M KCl solution at scan rate 100 mV/s. From the figure it is confirmed that, cathodic peak current increases with increase in the concentration of potassium ferricyanide. The graph of cathodic peak current against different concentrations of potassium ferricyanide shows a linear relationship as shown in the Fig. 3b. Cathodic peak current increases from 45.6 to 86.5  $\mu\text{A}$  with increase in the concentration of potassium ferricyanide from 1 to 3 mM.

### 3.3 Effect of pH

The pH of the supporting electrolyte is one of the main experimental parameters that can affect the voltammetric response of the potassium ferricyanide at CuO/GCE. Therefore, an optimum pH is required to maximize the intensity of redox peak currents. The electrochemical response of potassium ferricyanide at CuO/GCE is found to be pH dependent. Figure 4a shows the graph of cathodic peak current versus different pH of the acetate buffer solution (3.2 to 6.3) at a scan rate of 100 mV/s. From the graph it is clear that CuO/GCE show maximum anodic peak current at pH 5 due to the increased rate of reduction at this pH. The maximum cathodic peak current of CuO/GCE at pH 5 is found to be 47  $\mu\text{A}$ . Therefore, for the further analysis, pH 5 was selected. Figure 4b show a Plot of  $E^0$  v/s pH curve and it show linear relation of reduction potential and pH of the solution.

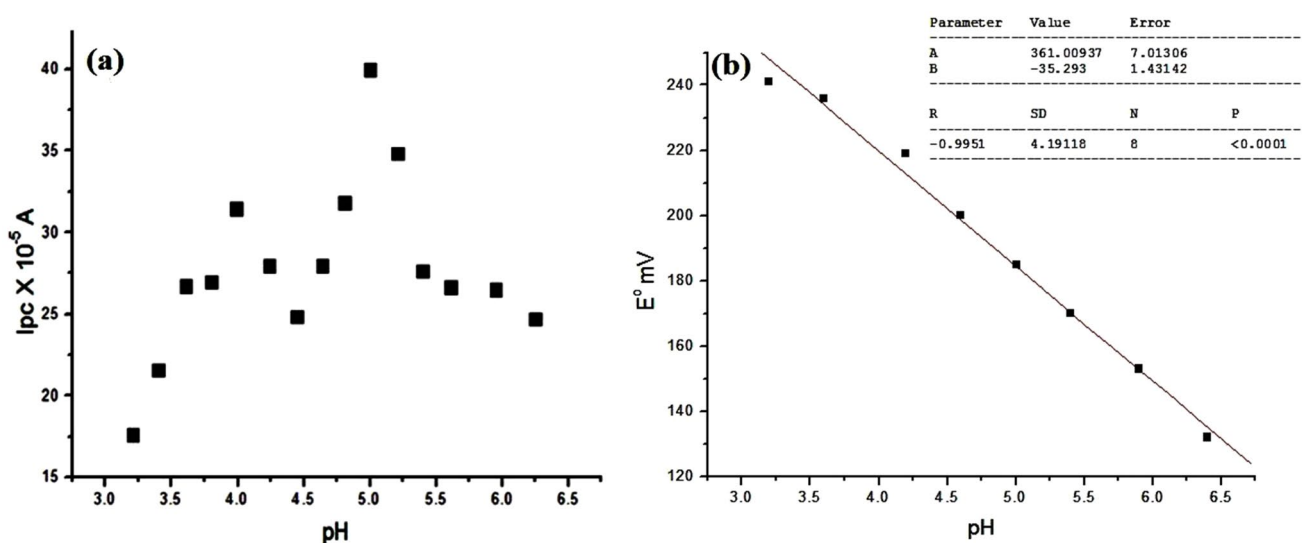


**Fig. 4** a Graph obtained for different pH values (3.2 to 6.3) in Acetate buffer solution at scan rate 100 mV/s. pH vs cathodic peak current b Plot of  $E^0$  v/s pH

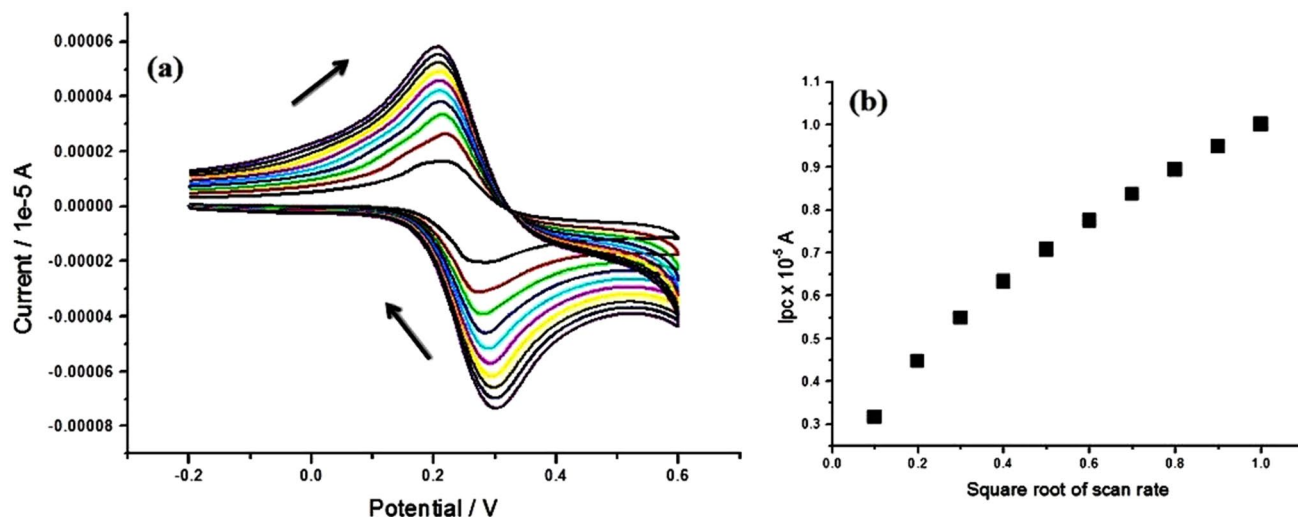


**Fig. 5** **a** Cyclic voltammograms for the effect of variation in the Scan rates from 0.1 to 1.0 V/s in Glassy carbon electrode **b** Graph of square root of scan rate vs cathodic peak current

### 3.4 Effect of scan rate

The scan rate increases with increase in peak current according to Randles-Sevcik's equation [45–48]. Figure 5a depicts the effect of scan rate on the cathodic peak current of 2 mM potassium ferricyanide in 1 M KCl solution. Increase in scan rate from 50 to 300 mV/s increases the cathodic peak current as shown in the voltammogram. The cathodic peak current increases from 17.4 to 57.7  $\mu A$  with the increase in scan rate from 50 to 300 mV/s. Figure 5b show the plot of square root of scan rate ( $v^{1/2}$ ) versus cathodic peak current. The plot show a straight line fitted linearly to calculate correlation coefficient for CuO/GCE and it is found to be 0.9843. This indicates that, the electron transfer reaction is adsorption controlled [26].

### 3.5 Preparation of dispersed copper oxide nanoparticles by a novel electrochemical method

It is very difficult to collect the deposited CuO nanoparticles as powder for further characterizations like XRD, SEM, UV–Visible spectroscopy and zeta potential analysis. We need to scratch the electrode surface to collect deposited CuO nanoparticles in powder form, but this may damage the electrode surface. Hence we establish a new instrumental setup to prepare CuO nanoparticles in powder form. The experimental setup requires a simple DC voltage source, beaker, magnetic stirrer and all the same chemicals used to deposit CuO nanoparticles on electrode. The 1.67 mM CuCl solution is added to 500 ml of 0.1 M NaOH solution taken in a beaker

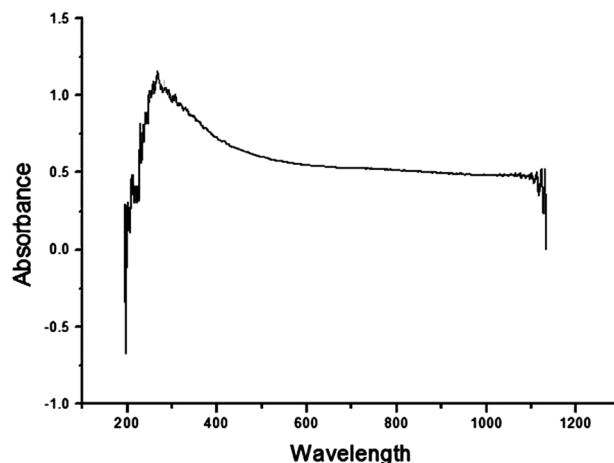


**Fig. 6** UV-Visible absorption spectra of prepared CuO nanoparticles

containing magnetic bead. Then beaker is placed on a magnetic stirrer and all the three electrodes are dipped into the beaker containing the above electrolyte and switch on the magnetic stirrer to maintain uniform agitation. Make sure that glassy carbon working electrode, platinum wire counter electrode and Ag/AgCl reference electrode are in good contact with the electrolyte. All the three electrodes are connected to DC voltage source and apply a reduction potential of +0.34 V. After few seconds CuCl present in 0.1 M NaOH come in contact with the surface of glassy carbon electrode and gets

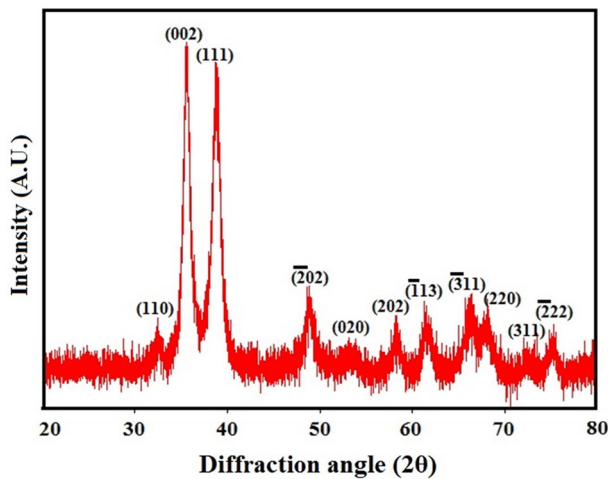


Fig. 7 XRD of as prepared CuO nanoparticles

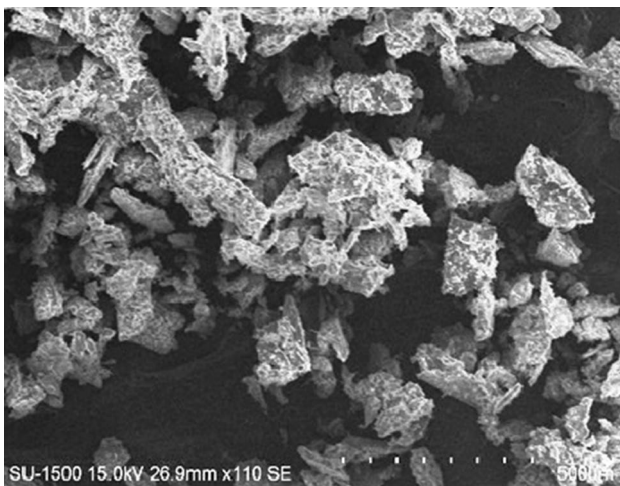


Fig. 8 SEM image of electrogenerated CuO nanoparticles

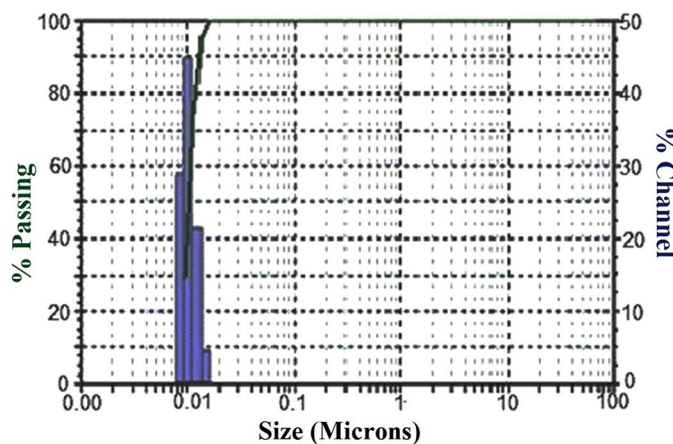


Fig. 9 Zeta potential of as prepared CuO nanoparticles

reduced to CuO nanoparticles. While reduction process, bubbles will form at the end surface of the glassy carbon electrode. These bubbles are due to the reduction reaction of CuO nanoparticles. After few minutes of reaction small black coloured CuO nanoparticles will generate inside a beaker dispersed in electrolyte. The electro generated CuO nanoparticles are filtered by whatman filter paper 5. The obtained CuO nanoparticles are washed with double distilled water 4–5 times to remove unconverted chlorides, hydroxides etc. Then powder is dried at room temperature and used for further characterizations to confirm the formation of CuO nanoparticles.

### 3.6 UV–visible absorption spectroscopy

The absorption peak is probably related to the electronic transition from valence band to conduction band due to the quantum size of the particle [49]. Peak at 288 nm is attributed by the formation of CuO nanoparticles as shown in Fig. 6. This band suggests the higher structural organization in the particle that takes place due to the donor–acceptor nature of metal ion, which leads to size-quantization effect due to band transition [50]. The broad absorbance peak is due to the nano structure of prepared CuO nanoparticles.

### 3.7 X-ray diffraction study

An XRD spectrum of electro-generated CuO nanoparticles is depicted in Fig. 7. It gives a single-phase with a monoclinic structure with lattice parameters  $a = 4.84 \text{ \AA}$ ,  $b = 3.47 \text{ \AA}$ ,  $c = 5.33 \text{ \AA}$  [49, 51]. Most of the structural or cell parameters, positions of peaks are in good agreement

Zeta Potential	
Mobility	4.55 $\mu\text{s/V/cm}$
Zeta Potential	58.29 mV
Charge	0.00042 fC
Polarity	Positive
Conductivity	3980 $\mu\text{S/cm}$

with the reported values. The peaks are broad due to the nano crystallinity, instrumental errors, strain etc. The average crystallite size of CuO nanoparticles is measured to be 2 nm using Scherrer formula [52].

### 3.8 Scanning electron microscope

The powder morphology of electro-generated CuO nanoparticles was investigated by using SEM. Figure 8 show a typical image of an electro generated copper oxide nanoparticles. The prepared CuO nanoparticles exhibit flake shapes with high degree of porosity and enhanced surface area. Therefore, due to the high surface area, the prepared CuO nanoparticles show excellent catalytic activities. Along with that, the prepared CuO nanoparticles also possess unusual properties due to their nano size, high reaction activity and efficient transmission channel for analyte molecules to reach the active sites, which will help to improve their stability and sensitivity in a significant way [53–57].

### 3.9 Zeta-potential and particle size analysis

Zeta-potential is the electrical potential developed at the solid–liquid interface in response to the relative movement of the nanoparticles and the solvent. The zeta-potential of CuO nanoparticles are studied by dispersing them in double distilled water. The zeta-potential of particles is a good indicator of their electrical potentials. Higher the zeta potential, the greater will be the surface potential of charged Particles [2]. The zeta potential of prepared CuO nanoparticles is found to be + 58.29 mV. Detailed output of the zeta-potential and the particle size distribution is shown Fig. 9. According to Zeta-potential analysis the prepared CuO nanoparticles have the average crystallite size of 1 nm which is in good agreement with crystallite size calculated using Scherrer formula by XRD spectrum.

## 4 Conclusion

We prepared CuO nanoparticles by electro-deposition and electro-generation at the same time using glassy carbon electrode by cyclic voltammetry method. The fabricated CuO/GCE proved to be a highly sensitive and stable electrode in determining the potassium ferricyanide. We also studied the effect of potential cycles, scan rate, concentration of analyte and pH on the cathodic peak current of ferricyanide. In the later part of the experiment we also electro-generated CuO nanoparticles for further characterization. The prepared CuO

nanoparticles exhibit excellent electro-catalytic properties due their high surface area and availability of large number of reaction sites in CuO/GCE. In future, the fabricated electrode can be a potential candidate in detecting environmentally toxic potassium ferricyanide in bleaching powder. We strongly believe that the fabricated modified CuO/GCE can also be the potential electrode for the determination of various bioactive organic molecules. Due to its low cost and ease of preparation the modified electrode seems to be an excellent candidate for further sensor development.

### Compliance with ethical standards

**Conflict of interest** On behalf of all authors, the corresponding author states that there is no conflict of interest.

## References

1. McCarrol WH, Ramanujachary KV (2005) Oxides: solid-state chemistry. In: King RB (ed) Encyclopedia of inorganic chemistry. Wiley, Hoboken, pp 4006–4053
2. Shashanka R, Kumara Swamy BE, Reddy S, Chaira D (2013) Synthesis of silver nanoparticles and their applications. *Anal Bioanal Electrochem* 5:455
3. Shashanka R, Kamacı Y, Taş R, Ceylan Y, Bülbül AS, Uzun O, Karaoglanlı AC (2019) Antimicrobial investigation of CuO and ZnO nanoparticles prepared by a rapid combustion method. *Phys Chem Res* 7:799
4. Nayak AK, Shashanka R, Chaira D (2016) Effect of nanosize yttria and tungsten addition to duplex stainless steel during high energy planetary milling. *IOP Conf Ser Mater Sci Eng* 115:012008
5. Shashanka R, Chaira D (2016) Effects of nano-Y<sub>2</sub>O<sub>3</sub> and sintering parameters on the fabrication of PM duplex and ferritic stainless steel. *Acta Metall Sin (Engl Lett)* 29:58
6. Liu X, Li X, Guan Z, Liu J, Zhao J, Yang Y, Yang Q (2011) Organosilica nanotubes: large-scale synthesis and encapsulation of metal nanoparticles. *Chem Commun* 47:8073
7. Shashanka R, Chaira D, Kumara Swamy BE (2015) Electrocatalytic response of duplex and yttria dispersed duplex stainless steel modified carbon paste electrode in detecting folic acid using cyclic voltammetry. *Int J Electrochem Sci* 10:5586
8. Veeresh Kumar GB, Rao CSP, Selvaraj N (2011) Mechanical and tribological behavior of particulate reinforced aluminum metal matrix composites—a review. *J Miner Mater Charact Eng* 10:59
9. Tatami J, Nakano H, Wakihara T, Komeya K (2010) Development of advanced ceramics by powder composite process. *KONA Powder Part J* 28:227
10. Anpo Masakazu, Shima Takahito, Kodama Sukeya, Kubokawa Yutaka (1987) Photocatalytic hydrogenation of propyne with water on small-particle titania: size quantization effects and reaction intermediates. *J Phys Chem* 91:4305
11. Shen YL, Fishencord E, Chawla N (2000) Correlating macrohardness and tensile behavior in discontinuously reinforced metal matrix composites. *Scripta Mater* 42:427



12. Shashanka R (2017) Synthesis of nano-structured stainless steel powder by mechanical alloying-an overview. *Int J Sci Eng Res* 8:588
13. Marco MD, Sadun C, Port M, Guilbert I, Couvreur P, Dubernet C (2007) Physicochemical characterization of ultrasmall superparamagnetic iron oxide particles (USPIO) for biomedical application as MRI contrast agents. *Int J Nanomed* 2:609
14. Yanhong L, Dejun W, Qidong Z, Min Y, Qinglin Z (2004) A study of quantum confinement properties of photogenerated charges in ZnO nanoparticles by surface photovoltage spectroscopy. *J Phys Chem B* 108:3202
15. Dulal SMSI, Won MS, Shim YB (2010) Characterisation of platinum nanoparticles electrodeposited on carbon felt. *J Sci Res* 2:303
16. Reddy S, Kumara Swamy BE, Aruna S, Mohan Kumar R, Shashanka H Jayadevappa (2012) Preparation of NiO/ZnO hybrid nanoparticles for electrochemical sensing of dopamine and uric acid. *Chem Sens* 2:1
17. Shashanka R, Chaira D, Kumara Swamy BE (2015) Electrochemical investigation of duplex stainless steel at carbon paste electrode and its application to the detection of dopamine, ascorbic and uric acid. *Int J Sci Eng Res* 6:1863
18. Shashanka R, Chaira D, Kumara Swamy BE (2016) Fabrication of yttria dispersed duplex stainless steel electrode to determine dopamine, ascorbic and uric acid electrochemically by using cyclic voltammetry. *Int J Sci Eng Res* 7:1275
19. Manasa G, Mascarenhas RJ, Basavaraja BM (2019) Sensitively-selective determination of Propyl Paraben preservative based on synergistic effects of polyaniline-zinc-oxide nano-composite incorporated into graphite paste electrode. *Colloids Surf B* 184:110529
20. Manasa G, Bhakta AK, Mekhalif Z, Mascarenhas RJ (2019) Voltammetric study and rapid quantification of resorcinol in hair dye and biological samples using ultrasensitive maghemite/MWCNT modified carbon paste electrode. *Electroanalysis* 31:1363
21. Erady V, Mascarenhas RJ, Satpati AK, Bhakta AK, Mekhalif Z, Delhalle J, Dhason A (2019) Carbon paste modified with Bi decorated multi-walled carbon nanotubes and CTAB as a sensitive voltammetric sensor for the detection of Caffeic acid. *Microchem J* 146:73
22. Bukkitgar SD, Shetti NP, Kulkarni RM, Reddy KR, Shukla SS, Saji VS, Aminabhavi TM (2019) Electro-catalytic behavior of Mg-doped ZnO nano-flakes for oxidation of anti-inflammatory drug. *J Electrochem Soc* 166:B3072
23. Bukkitgar SD, Shetti NP (2016) Electrochemical behavior of anticancer drug 5-fluorouracil at carbon paste electrode and its analytical application. *J Anal Sci Technol* 7:1
24. Shetti NP, Nayak DS, Malode SJ, Kulkarni RM, Kulkarni DB, Teggi RA, Joshi VV (2017) Electrooxidation and determination of flufenamic acid at graphene oxide modified carbon electrode. *Surf Interfaces* 9:107
25. Shetti NP, Nayak DS, Malode SJ, Reddy KR, Shukla SS, Aminabhavi TM (2019) Electrochemical behavior of flufenamic acid at amberlite XAD-4 resin and silver-doped titanium dioxide/amberlite XAD-4 resin modified carbon electrodes. *Colloids Surf B* 177:407
26. Zhi LW, Qin LY (2009) Nonenzymatic biosensor based on Cu<sub>2</sub>O nanoparticles deposited on polypyrrole nanowires for improving detection range. *Sensor Actuat B* 141:147
27. Kumar S, Bukkitgar SD, Singh S, Pratibha V, Singh KR, Reddy NP, Shetti V, Reddy V, Sadhu S Naveen (2019) Electrochemical sensors and biosensors based on graphene functionalized with metal oxide nanostructures for healthcare applications. *Chem Select* 4:5322
28. Dakshayini BS, Reddy KR, Mishra A, Shetti NP, Malode SJ, Basu S, Naveen S, Raghu AV (2019) Role of conducting polymer and metal oxide-based hybrids for applications in amperometric sensors and biosensors. *Microchem J* 147:7
29. Shikandar DB, Shetti NP, Kulkarni RM, Kulkarni SD (2018) Silver-doped titania modified carbon electrode for electrochemical studies of furantril. *ECS J Solid State Sci Technol* 7:Q3215
30. Shetti NP, Nayak DS, Bukkitgar SD (2016) Electrooxidation of antihistamine drug methdilazine and its analysis in human urine and blood samples. *Cogent Chem* 2:1153274
31. Shettia NP, Malode SJ, Nayak DS, Aminabhavi TM, Reddy KR (2019) Nanostructured silver doped TiO<sub>2</sub>/CNTs hybrid as an efficient electrochemical sensor for detection of anti-inflammatory drug, cetirizine. *Microchem J* 150:104124
32. Shetti NP, Malode SJ, Bukkitgar SD, Bagihalli GB, Kulkarni RM, Pujari SB, Reddy KR (2019) Electro-oxidation and determination of nimesulide at nanosilica modified sensor. *Mater Sci Energy Technol* 2:396
33. Kulkarni DR, Malode SJ, Prabhu KK, Ayachit NH, Kulkarni RM, Shetti NP (2020) Development of a novel nanosensor using Ca-doped ZnO for antihistamine drug. *Mater Chem Phys* 246:122791
34. Shetti NP, Shanbhag MM, Malode SJ, Srivastava RK, Reddy KR (2020) Amberlite XAD-4 modified electrodes for highly sensitive electrochemical determination of nimesulide in human urine. *Microchem J* 153:104389
35. Shetti NP, Malode SJ, Nayak DS, Bukkitgar SD, Bagihalli GB, Kulkarni RM, Reddy KR (2020) Novel nanoclay-based electrochemical sensor for highly efficient electrochemical sensing nimesulide. *J Phys Chem Solids* 137:109210
36. Honakeri NC, Malode SJ, Kulkarni RM, Shetti NP (2020) Electrochemical behavior of diclofenac sodium at coreshell nanostructure modified electrode and its analysis in human urine and pharmaceutical samples. *Sens Int* 1:100002
37. Bhakta AK, Kumari S, Hussain S, Martis P, Mascarenhas RJ, Delhalle J, Mekhalif Z (2019) Synthesis and characterization of maghemite nanocrystals decorated multi-wall carbon nanotubes for methylene blue dye removal. *J Mater Sci* 54:200
38. Sharpe AG (1976) The chemistry of cyano complexes of the transition metals. Academic Press, London
39. Niranjana E, Raghavendra Naik R, Kumara Swamy BE, Sherigara BS, Jayadevappa H (2007) Studies on adsorption of Triton X-100 at carbon paste and ceresin wax carbon paste electrodes and the enhancement effect in dopamine oxidation by cyclic voltammetry. *Int J Electrochem Sci* 2:923
40. Bukkitgar SD, Shetti NP, Malladi RS, Reddy KR, Kalanur SS, Aminabhavi TM (2020) Novel ruthenium doped TiO<sub>2</sub>/reduced graphene oxide hybrid as highly selective sensor for the determination of amroxol. *J Mol Liq* 300:112368
41. Manasa G, Mascarenhas RJ, Satpati AK, Basavaraja BM, Kumar S (2018) An electrochemical Bisphenol F sensor based on ZnO/G nano composite and CTAB surface modified carbon paste electrode architecture. *Colloids Surf B* 170:144
42. Rahbar N, Parham H (2013) Carbon paste electrode modified with CuO-nanoparticles as a probe for square wave voltammetric determination of atrazine. *Jundishapur J Nat Pharm Prod* 8:118
43. Amra S, Bataille T, Bacha SB, Bourouina M, Hauchard D (2020) Nanostructured modified carbon paste electrode as voltammetric sensor for isoproturon trace analysis in wate. *Electroanalysis*. <https://doi.org/10.1002/elan.201900083>
44. Chandrashekar BN, Kumara Swamy BE, Pandurangachar M, Shankar SS, Gilbert O, Manjunatha JG, Sherigara BS (2010)

- Electrochemical oxidation of dopamine at polyethylene glycol modified carbon paste electrode: a cyclic voltammetric study. *Int J Electrochem Sci.* 5:578
45. Hareesha N, Manjunatha JG, Raril C, Tigari G (2019) Design of novel surfactant modified carbon nanotube paste electrochemical sensor for the sensitive investigation of tyrosine as a pharmaceutical drug. *Adv Pharm Bull* 9:135
  46. Amrutha BM, Manjunatha JG, Aarti Bhatt S, Hareesha N (2019) Electrochemical analysis of evans blue by surfactant modified carbon nanotube paste electrode. *J Mater Environ Sci* 10:668
  47. Manjunatha JG (2017) A new electrochemical sensor based on modified carbon nanotube mixture past electrode for voltammetric determination of resorcinol. *Asian J Pharm Clin Res* 10:295
  48. Manjunatha JG (2018) A novel poly (glycine) biosensor towards the detection of indigo carmine: a voltammetric study. *J Food Drug Anal* 26:292
  49. Topnani N, Kushwaha S, Athar T (2009) Wet synthesis of Copper oxide nanopowder. *Int J Green Nanotechnol Mater Sci Eng* 1:M67
  50. Vossmeier T, Katsikas L, Gienig M, Popovic IG, Diesner K, Chemseddine A, Eychmiiller A, Weller H (1994) CdS nanoclusters: synthesis, characterization, size dependent oscillator strength, temperature shift of the excitonic transition energy, and reversible absorbance shift. *J Phys Chem* 98:7665
  51. Harikrishnan S, Kalaiselvam S (2012) Preparation and thermal characteristics of CuO–oleic acid nanofluids as a phase change material. *Thermochim Acta* 533:46
  52. Klug H, Alexander L (1962) X-ray diffraction procedures. Wiley, New York
  53. Shashanka R, Kumara Swamy BE (2020) Biosynthesis of silver nanoparticles using leaves of acacia melanoxylon and their application as dopamine and hydrogen peroxide sensors. *Phys Chem Res* 8:1
  54. Mumtaz A, Rehman S, Hasanain SK (2011) Size effects on the magnetic and optical properties of CuO nanoparticles. *J Nanopart Res* 13:2497
  55. Le W-Z, Liu Y-Q (2009) Preparation of nano-copper oxide modified glassy carbon electrode by a novel film plating/potential cycling method and its characterization. *Sens Actuat B* 141:147
  56. Shashanka R (2019) Non-lubricated dry sliding wear behavior of spark plasma sintered nano-structured stainless steel. *J Mater Environ Sci* 10:767
  57. Shashanka R (2018) Effect of sintering temperature on the pitting corrosion of ball milled duplex stainless steel by using linear sweep voltammetry. *Anal Bioanal Electrochem* 10:349

**Publisher's Note** Springer Nature remains neutral with regard to jurisdictional claims in published maps and institutional affiliations.